Asian Journal of Chemistry; Vol. 36, No. 12 (2024), 2765-2771

ASIAN JOURNAL OF CHEMISTRY

https://doi.org/10.14233/ajchem.2024.32576

# Green Biosynthesis of Silver Nanoparticles using Aqueous Extract of *Pseuderanthemum reticulatum* Leaves and their Antioxidant and Anti-Aging Activities

S. Margrat Sheela*, J. Rosaline Vimala, M. Stella Bharathy, A. Agila, J. Theeshma and J. Santhiya

Department of Chemistry, Holy Cross College (Autonomous), (Affiliated to Bharathidasan University), Tiruchirappalli-620002, India

*Corresponding author: E-mail: msheela86@gmail.com

*Received*: 26 August 2024; *Accepted*: 4 October 2024; *Published online*: 30 November 2024; AJC-21816

The plant based synthesis of nanoparticles are highly recommended because of its low toxicity, low cost and eco-friendly nature. In present work, synthesis of silver nanoparticles (AgNPs) involves a bioreduction technique using the aqueous extract derived from the leaves of *Pseuderanthemum reticulatum*. The synthesized AgNPs were characterized by UV-visible, FT-IR, EDAX, XRD, SEM, TEM, zeta potential analysis and particle size analyzing techniques. The results showed the characteristic absorbance peak at 404 nm in the UV-visible spectrum, the strong signals observed in the EDAX spectrum and the other characterization confirmed the formation of AgNPs with an average particle size of 17.83 nm. The *in vitro* antioxidant activity of AgNPs by DPPH method results revealed that they have greater radical scavenging capacity with the $IC_{50}$ value of 101.5 µg/mL. Additionally, the anti-aging activity was also determined by collagenase inhibition assay. The biogenic AgNPs established its strong anti-aging efficacy as demonstrated by their inhibitory capacity against *Actinomyces israelii* (collagenase enzyme). Since, the AgNPs synthesized using aqueous extract of *P. reticulatum* exhibited leaves excellent antioxidant and anti-aging activity, it can be promising choice for various biological applications.

**Keywords: *P. reticulatum*, Silver nanoparticles, Antioxidant activity, Anti-aging activity, Collagenase inhibition assay.**

## INTRODUCTION

Today nanotechnology is one of the emerging multidisciplinary fields in the modern research and deals with the synthesis of materials in nanoscale (1-100 nm) dimension. These nanoparticles gained more attention because of their unique properties such as their extremely small size, large surface to volume ratio, catalytic activity, thermal conductivity, electrical properties, non-linear optical performance, stability, *etc.* [1-3]. The metal oxide nanoparticles have distinctive chemical and physical properties attributable to their size and high density of corner surfaces and are utilized in sensors, fuel cells and coatings [4,5].

There are different methods available for the synthesis of metal oxide nanoparticles, which includes the physical method, chemical method and green synthesis [6-8]. Synthesis of nanoparticles using plant extract received much more attention due to its cost effectiveness, eco-friendly nature and these mostly used in the medicinal fields for curing diseases [9]. Green mediated silver nanoparticles (AgNPs) have a number of advantages over other metal nanoparticles, including being easily accessible, low-cost, environmental friendly and having less toxicity. Moreover, AgNPs produced biologically exhibit unique characteristics, such as hydrophilicity, large surface area and improved stability [10].

The synthesis of silver nanoparticles using extract of different parts such as leaf, roots, seed, fruits and stem, *etc*. of the medicinal plants have been widely reported in the literature [11-14]. The green synthesis utilizes the extracts as sources of capping and reducing agents in the synthesis of AgNPs, and suggested that the biomolecules, especially secondary metabolites present in these extracts, could reduce the Ag ions [15]. In current years, the free radical chemistry attained more attention in the field of medicinal research. In nature, many plants have natural antioxidants, which contain active anthocyanins, phenolic compounds and flavonoids [16,17]. Similarly, nanoparticles present a promising option for facilitating drug passage across the blood-brain barrier (BBB), potentially enhancing treatment efficacy and reducing adverse effects [18].

*Pseuderanthemum reticulatum* is an ornamental plant and used in traditional medicine to take care of fever, headache,

cold and back pain [19] and this plant is cultivated in different parts of the world to increase the aesthetic value of the gardens. Thus, in present study, a biosynthesis approach is adopted for the synthesis of AgNPs using leaves of *P. reticulatum*. The synthesized Ag-NPs were characterized through UV-visible, FT-IR, EDAX, XRD, SEM, TEM, zeta potential analysis and particle size analyzing techniques. Moreover, the synthesized nanoparticles were also evaluated for their antibacterial, antioxidant and anti-aging potency.

## EXPERIMENTAL

**Collection of leaves:** Fresh leaves of *Pseuderanthemum reticulatum* plant was collected from the garden of the premises of college and authenticated by the Department of Botany, Holy Cross College, Tiruchirappalli, India. With the help of a sterile medical blade, the fresh leaves were cut into the little pieces and then rinsed thoroughly with distilled water to remove dust and other foreign materials before drying in shade. The well-dried leaves were ground at 25 ºC for aqueous extraction. Around 30 g of fine powder plant material was added to 500 mL flasks with distilled water to generate 200 mL of aqueous solution. Flasks were sonicated for 10 min and shaken at 200 rpm in a 37 ºC incubator for 24 h. The extract was filtered with Whattman filter paper to eliminate remaining particles.

**Green synthesis of silver nanoparticles:** The silver nanoparticles were synthesized using the aqueous extract of derived from the leaves of *P. reticulatum* and $AgNO_3$ solution (2 mM) by bioreduction method. The synthesis was optimized using UV-visible spectrophotometer with respect to salt to precursor ratio, reaction time, pH and temperature to maximize the silver nanoparticles yield. The optimization was performed in triplicate for better reproducibility.

**Optimization of salt to precursor ratio:** To optimize the salt to precursor ratio, $AgNO_3$ solution and plant extract (AEPR) in different ratios (1:1, 1:4, 2:3, 3:2, 4:1) were investigated. In order to determine the optimal ratio for achieving optimum synthesis of AgNPs, the spectrophotometer was used to examine the UV absorption spectra of the solutions at various ratios.

**Optimization of time:** The UV absorption peaks of the reacting solutions were measured using UV-visible spectrophotometer at different in travels of time. The UV spectrum plot was drawn and compared to find the optimum time required for completion of the reaction (30 to 150 min).

**Optimization of pH:** The optimization of pH of the solution for the synthesis of AgNPs was carried out by varying pH (from 1 to 13) of the solution by fixing the salt to precursor ratio and time. The pH of the solutions was adjusted with HCl and/or liquid ammonia using pH meter.

**Optimization of temperature:** The optimum temperature for the synthesis of AgNPs was performed at different temperatures *viz*. 40 ºC, 50 ºC, 60 ºC and 70 ºC, respectively. For each temperature, the UV absorption spectrum was observed.

**Characterization:** The synthesized silver nanoparticles using AEPR was optimized with the parameters such as salt to precursor ratio (1:4), temperature (40 ºC), pH 7 and time (30 min). Then it was subjected to the following characterization. The UV-visible absorption spectrum of the synthesized AgNPs was analyzed using UV-visible spectrometer (Shimadzu UV-2700). The FT-IR spectrum was recorded using a Fourier-transform infrared (FTIR) spectrometer (Spectrum One System, Perkin-Elmer, Waltham) to identify the potential bioactive functional groups present in the extract, which are responsible for the reduction and capping of the silver nanoparticles. JEOL-JEM 2100 (Tokyo, Japan) instrument was used for the elemental analysis and chemical characterization. The scanning electron microscopy (SEM) analysis of synthesized AgNPs was carried out using a Hitachi S-4500 SEM machine, while the size and shape were confirmed by transmission electron microscopy (TEM) using Gatan Ultrascan 4000 digital camera attached to a JEOL 2010 transmission electron microscope running at 20 kV. The crystalline nature of the synthesized nanoparticles was analyzed using the X-ray diffraction technique (XRD), which was recorded using XRD, D8 Advance (Bruker, Germany), operated at 40 kV, 40 mA, with Cu$K\alpha$ radiation, at a scanning rate of 6º/min, step size 0.02, over the 2θ range of 20-80º. The particle size distribution and zeta potential were analyzed using zetasizer Nano-ZS90 (Malvern Instruments, UK).

***In vitro* antioxidant activity by DPPH method:** A 300 µL of synthesized AgNPs at varying concentrations were mixed with 100 µL of DPPH (2,2-diphenyl-1-picrylhydrazyl) solution of 0.1 mM concentration. The solutions were vigorously shaken and left at room temperature for 30 min. Subsequently, the absorbance of each solution was measured at 517 nm using a UV-vis spectrophotometer and ascorbic acid used as a reference. The DPPH radical scavenging ability of the synthesized AgNPs was calculated using the following formula [20]:

$$\text{DPPH radical scavenging activity } (\%) = \left(1 - \frac{A_s}{A_c}\right) \times 100$$

where $A_s$ is the absorbance of sample solution containing AgNPs; $A_c$ is the absorbance of the control solution without AgNPs (containing only DPPH and solvent).

***In vitro* antianti-aging activity by collagenase inhibition assay:** The assay was performed in 50 mM tricine buffer (pH 7.5 with 400 mM NaCl and 10 mM $CaCl_2$). Collagenase from *Actinomyces israelii* (ChC, EC.3.4.23.3) was purchased from MTCC, Chandigarh, India. The synthetic substrate N-[3-(2-furyl)acryloyl]-Leu-Gly-Pro-Ala (FALGPA) was dissolved in tricine buffer (2 mM). The test samples were incubated with the enzyme in buffer for 15 min before adding substrate to start the reaction. The final reaction mixture (150 µL total volume) contained tricine buffer, 0.8 mM FALGPA, 0.1 units ChC and 25 µg test extracts. Negative controls were performed with water. The absorbance was measured at 335 nm immediately after adding substrate using a microplate reader in a 96 well microtiter plates. The inhibition percentage was calculated according to the following formula:

$$\text{Collagenase inhibition activity } (\%) = \left(1 - \frac{S_{abs} - Sb_{abs}}{C_{abs} - Cb_{abs}}\right) \times 100$$

where S = sample test absorbance; Sb = sample blank absorbance, C = positive control absorbance; and Cb = negative control absorbance.

## RESULTS AND DISCUSSION

The silver nanoparticles (AgNPs) were synthesized using aqueous extract derived from the leaves of *Pseuderanthemum reticulatum* (AEPR) by bioreduction method. The formation of AgNPs was observed by change in the colour change of the solution after the addition of AEPR to $AgNO_3$ solution. The colour change of the solution is due to the reduction of silver ions. The progress of reduction of was evaluated by UV-visible spectra using the colloidal solution of AgNPs.

**Optimization of synthesis of AgNPs:** The UV-visible absorption spectrum of various material to precursor ratio were recorded and overlay was plotted (Fig. 1). The optimal concentration ratio for the material to precursor ratio was found to be 1:4, whih is due to the fact that a higher precursor concentration (AEPR) induces a higher concentration of secondary metabolites including alkaloids, flavonoids, anthocyanins and tannins, all of which readily reduce the silver ions [21]. The reaction time for the synthesis of AgNPs was optimized by increasing the reaction time from 30 to 180 min and the corresponding UV-visible absorption spectrum of the AgNPs formed in the reaction medium was recorded (Fig. 1b). From the optimization overlay plot, it was observed that by increasing the reaction time, the UV-visible peak absorption also increases. It was shown that the optimum time for the synthesis of AgNPs was found to be 60 min and after that the stability of AgNPs was decreased therefore, the absorption peak also decrease due to the forma-tion of colloidal solution.

The optimization of pH of the reaction medium was carried out by varying the pH (1, 3, 5, 7, 9 and 11) under optimized metal to precursor ratio (1:4) and time (60 min). The UV-visible absorption spectrum obtained for each pH were measured and are shown in Fig. 1c. The optimal condition for the complete reduction of AgNPs was observed to be at pH = 5, which is slightly acidic medium. In literature, it was reported that the synthesis AgNPs takes place in alkaline medium (pH 9) [22]. The stability of the nanoparticles is directly related to the pH. Since all the nanoparticles are stable at or around their isoelectric point, changes in pH can alter the double-layer characteristics, increasing or decreasing the probability of flocculation or coag-ulation. It is also reported that AgNPs exhibited an effective charge change in aqueous conditions, from positive

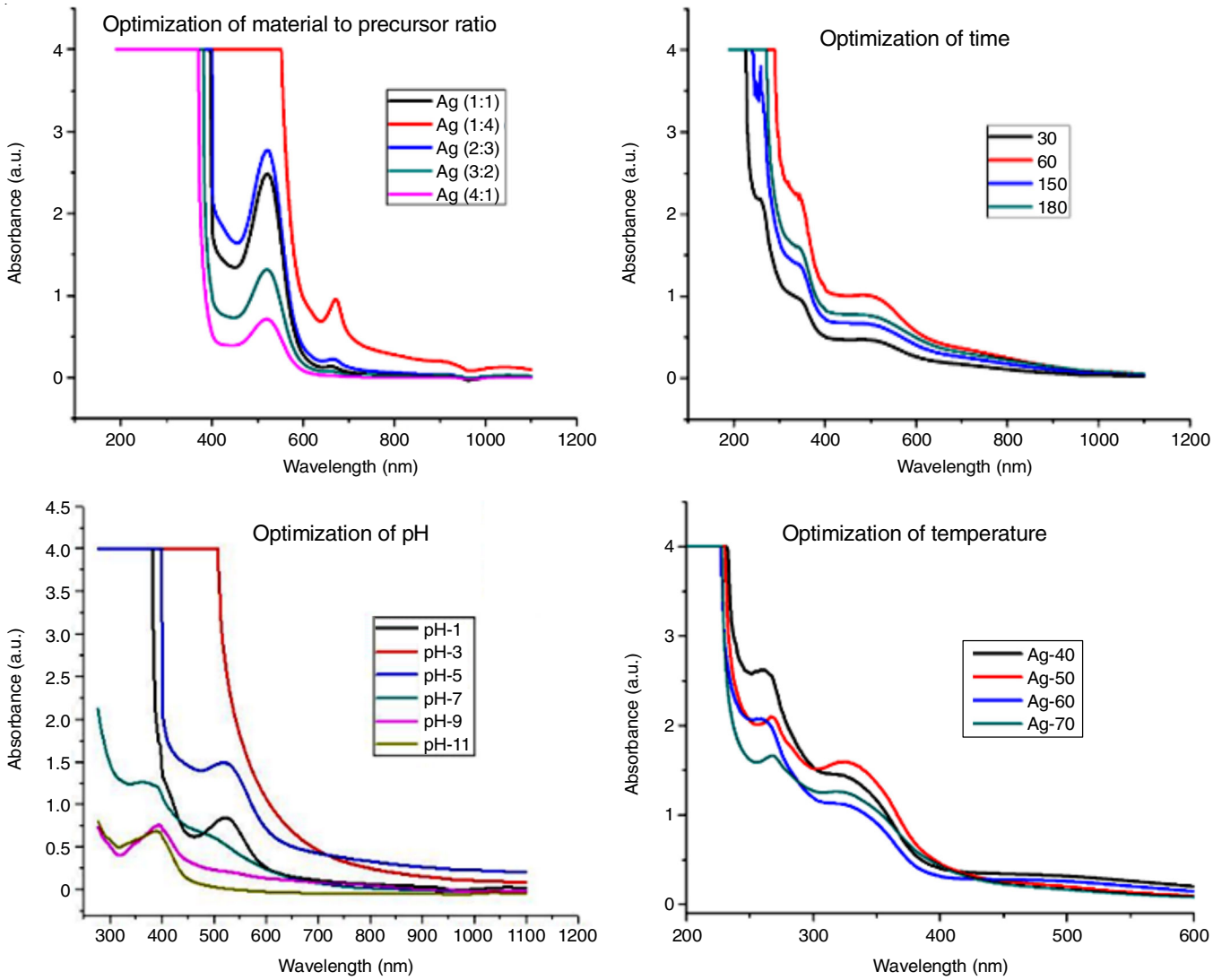


Fig. 1. Optimization of synthesis of *P. reticulatum* leaves mediated AgNPs

(in low pH) to negative (at high pH), with an isoelectric point between them [23]. Temperature is another important parameter because it controls the nucleation process in nanoparticle synthesis [24]. The optimum temperature required for the synthesis of AgNPs was studied by performing the AgNP synthesis at different temperatures (40 ºC, 50 ºC, 60 ºC and 70 ºC) by maintaining the other optimized parameters kept constant and the corresponding UV absorbance was recorded (Fig. 1d). The results show that the maximum absorbance observed for the formation of AgNPs was occured at 50 ºC. Initially, the temperature increases from 40 ºC to 50 ºC, the absorbance for the formation of AgNPs also increases. The temperatures at 60 ºC and 70 ºC, a slight decrease in the absorption was observed, which is due of the formation of crystal growth around the nucleus [25].

**UV-visible spectral studies:** The synthesized AgNPs exhibit strong absorption in the visible region due to the surface plasmon resonance. The UV-visible spectrum of AgNPs synthesized using AEPR shows a characteristic absorbance peak near 404 nm, which confirmed the formation of AgNPs [26]. The smaller wavelength of absorption indicates the formation of smaller sized nanoparticles [27]. In the UV spectrum, the other peaks around 500-600 nm are due to the presence of some secondary metabolites present in the extract (anthocyanins 504 nm and 533 nm) (Fig. 2).

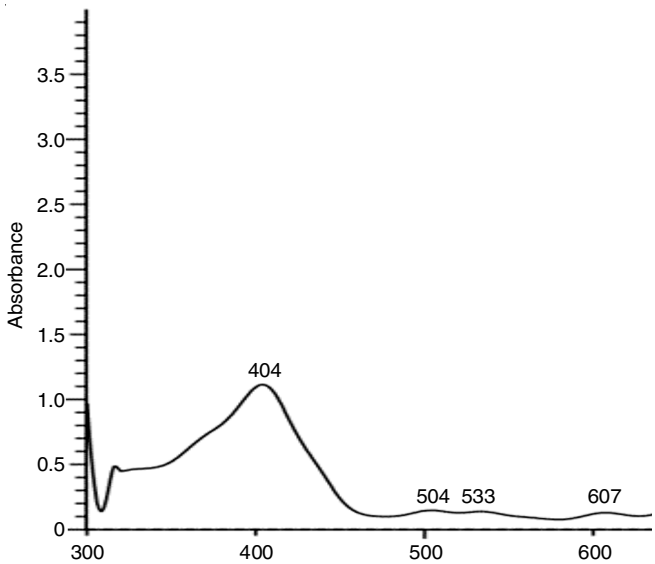


Fig. 2. UV-visible spectrum of *P. reticulatum* leaves mediated AgNPs

**FT-IR spectral studies:** The synthesized AgNPs were analyzed using FT-IR spectrophotometer to identify the possible interactions exist between the AgNPs and bioactive functional groups which are responsible for the reduction of silver ions. This is also used to predict the capping materials present in AgNPs [15]. The FT-IR spectrum of AgNPs synthesized using AEPR is shown in Fig. 3, which revealed that the absorption frequencies at 696.13, 600.28 and 556.91 $cm^{-1}$ confirmed the metal-oxygen bond of AgNPs. The strong carbonyl absorption peaks at 1637.73 $cm^{-1}$ indicates the participation of some flavonoid group of compounds (C-O stretching of aliphatic ether) [28] involved in the synthesis of AgNPs.

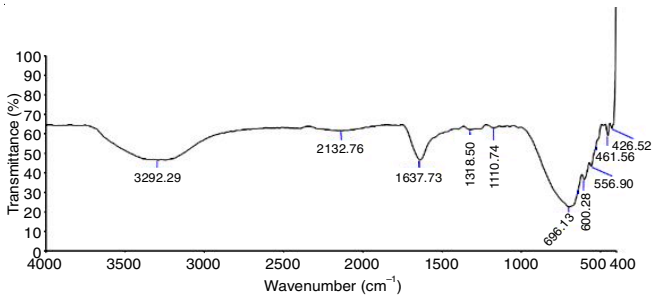


Fig. 3. FT-IR spectrum of *P. reticulatum* leaves mediated AgNPs

**Morphology studies:** In the EDAX spectrum, the distinct peaks were observed between 2.8-3.6 keV which corresponds to silver, thus the strong signals observed in the EDAX spectrum confirmed the formation of AgNPs [29]. In addition to silver, peaks corresponding to carbon (C) and oxygen (O) were detected in the spectrum (Fig. 4), indicating the presence of metal-oxygen bonds and other phytoconstituents involved in the stability of AgNPs.

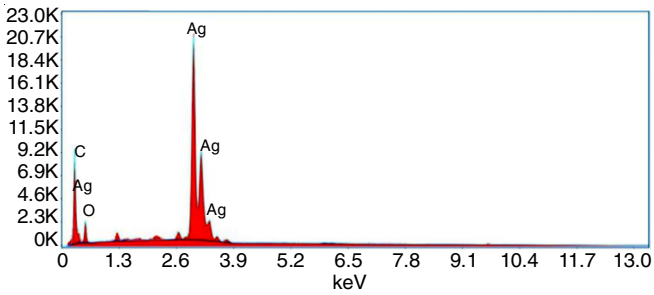


Fig. 4. EDAX spectrum of *P. reticulatum* leaves mediated AgNPs

The SEM images of AgNPs synthesized using AEPR were taken at 25,000X and 40,000X magnifications. The SEM images (Fig. 5) show that the AgNPs are in spherical, round, cuboidal and triangular shapes with smooth surface and the size of the particles around 10-40 nm.

**TEM studies:** The TEM images of AgNPs obtained using AEPR is shown in Fig. 6. The utilization of plant extracts in the synthesis not only enhances the pharmacological characteristics of the AgNPs but also regulates their size and structure [30]. The synthesized AgNPs mostly appear in spherical, truncated triangles, cuboidal and decahedral shapes as evidenced by the TEM images and the average size was found to be 17.83 nm.

**XRD studies:** The crystalline structure of nanoparticles is often assessed by XRD analysis and the particle size can be calculated using Scherrer's formula based on the peak width observed in the XRD data. The peaks observed in the XRD spectrum (Fig. 7) are extremely sharp and four distinct diffraction peaks at 35.94º, 47.24º, 62.60º and 67.68º with the 2θ values correspond to the plane (1 1 1), (2 0 0), (2 2 0) and (3 1 1), respectively [31] (JCPDS file no. 84-0713 and 04-0783) are observed. These results indicate that synthesized AgNPs are face centred cubic (fcc) and crystalline in nature.

**Zeta potential and DLS particle size:** The zeta potential measured for the synthesized AgNPs is shown in Fig. 8 and the zeta potential value -19.1 mV, signifying the presence of

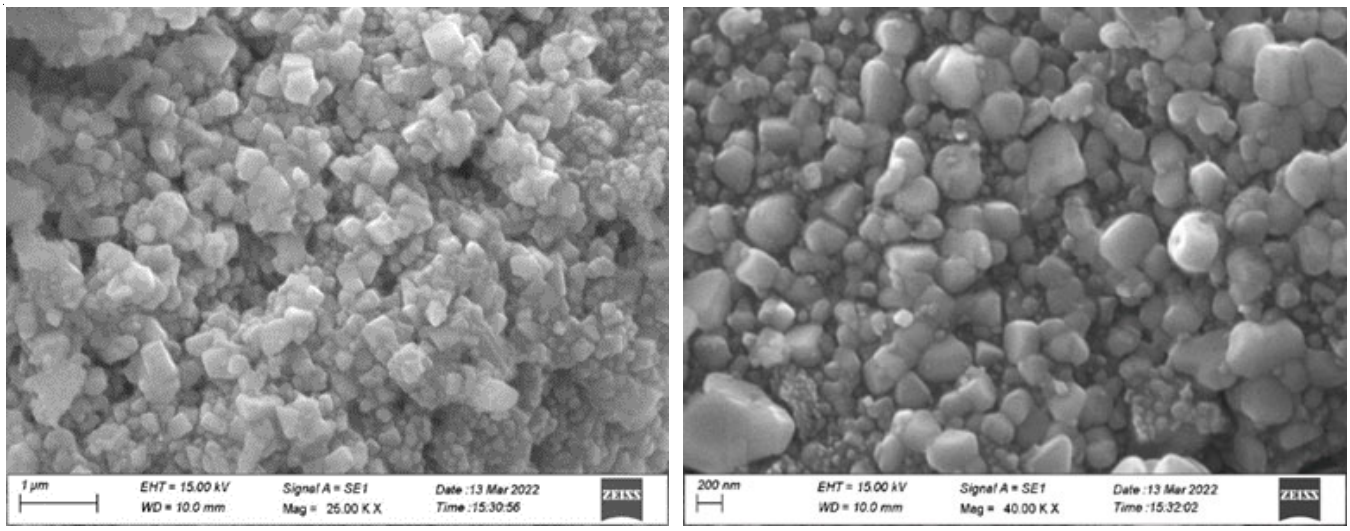


Fig. 5. SEM images of *P. reticulatum* leaves mediated AgNPs

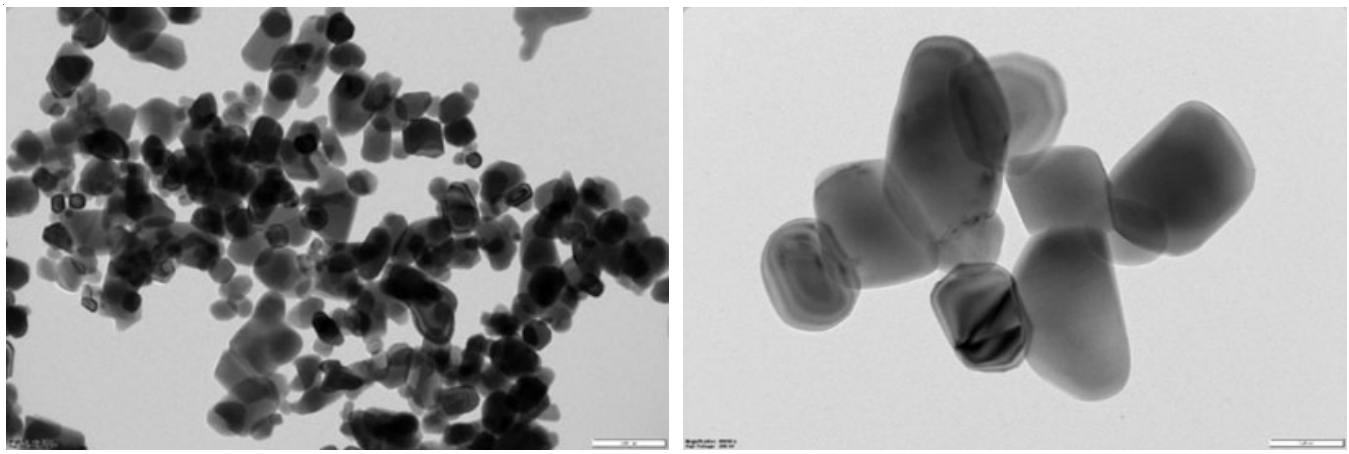

Fig. 6. TEM images of *P. reticulatum* leaves mediated AgNPs

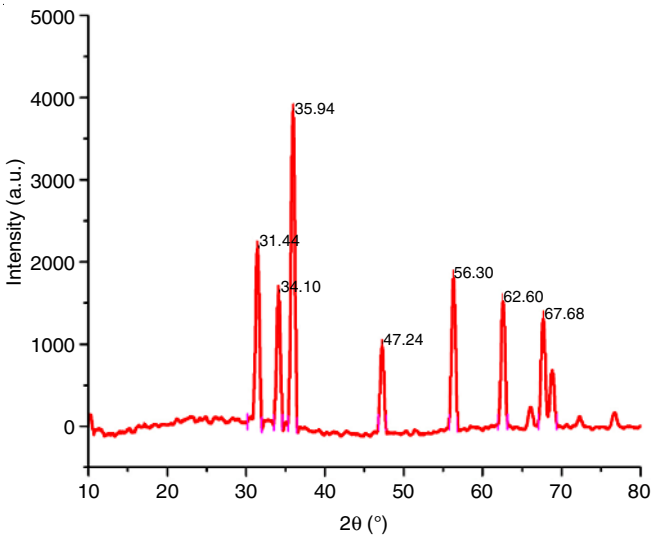


Fig. 7. XRD spectrum of *P. reticulatum* leaves mediated AgNPs

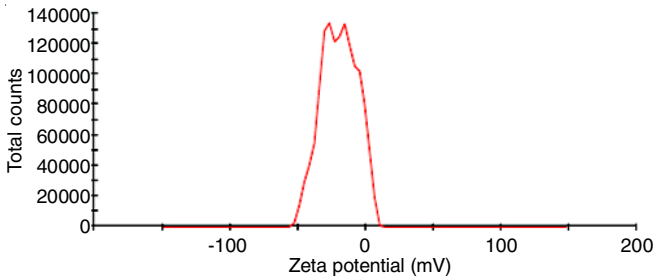


Fig. 8. Zeta potential of *P. reticulatum* leaves mediated AgNPs

repulsion among the synthesized nanoparticles, which further increases the stability of the formulation. It is evident that the AgNPs are polydisperse in nature, due to its high negative zeta potential; thus, the electrostatic repulsive force between them results in the prevention of agglomeration of the nanoparticles and is also very much helpful for long-term stability in the solution [32]. The particle sized distribution of the synthesized AgNPs is in the range from 10 nm to 40 nm, and the median diameter (taken as average particle diameter) is about 17.83 nm, being deduced from Fig. 9, which shows a relatively broad size distribution.

***In vitro* antioxidant activity:** The radical scavenging capacity of *in vitro* antioxidant activity was evaluated using the DPPH method, indicating remarkable antioxidant activity. At 500 mg/mL, the extract demonstrated a free radical scavenging ability of 64.99%. The $IC_{50}$ value, indicating the concentration

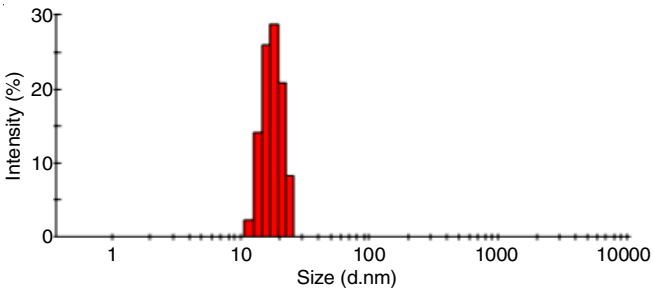


Fig. 9. Particle size distribution of biosynthesized AgNPs

required to reduce the DPPH concentration by 50%, was determined to be 101.5 mg/mL. The free radical inhibition percentage AEPR at different concentrations is shown in Fig. 10.

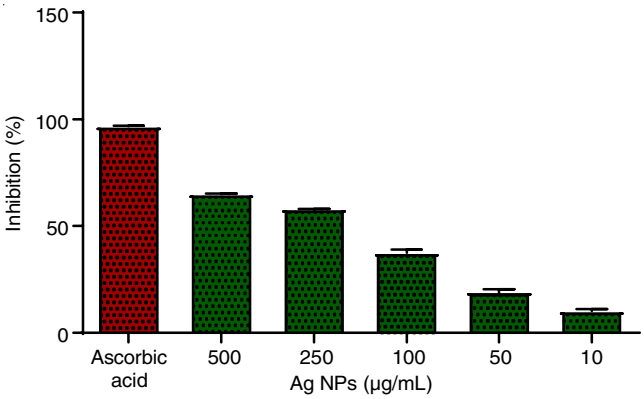


Fig. 10. Percentage of inhibition of DPPH by biosynthesized AgNPs

**Anti-aging activity of AgNPs by collagenase inhibition assay:** The anti-aging activity of biosynthesized AgNPs was studied by collagenase inhibition assay. The result of anti-collagenase activity is shown in Table-1 and the $IC_{50}$ value was found to be 67.36 mg/mL. The maximum inhibition of AgNPs was observed at 500 mg/mL (42.53%, Fig. 11), which shows the dose dependent inhibition of enzymes, attributing the conformational change in collagenase induced by the synergistic effect of phenolic compounds and flavonoids groups present in the aqueous extract derived from the leaves of *P. reticulatum*. Thus, the anti-collagenase activity results showed that the AEPR is effective towards anti-ageing.

TABLE-1
ANTI-COLLAGENASE ACTIVITY RESULTS ASSAY DATA OF BIOSYNTHESIZED AgNPs AT DIFFERENT CONCENTRATIONS

| Sample concentration (µg/mL) | OD Value at 335 nm (in triplicates) | | |
|---|---|---|---|
| Control | 0.952 | 0.929 | 0.913 |
| 500 | 0.533 | 0.546 | 0.526 |
| 250 | 0.770 | 0.760 | 0.726 |
| 100 | 0.886 | 0.828 | 0.815 |
| 50 | 0.901 | 0.903 | 0.925 |
| 10 | 0.994 | 1.342 | 1.542 |

## Conclusion

Silver nanoparticles (AgNPs) synthesized from the aqueous extract of *Pseuderanthemum reticulatum* leaves (AEPR) through bioreduction method was successfully accomplished. The UV-vis, FT-IR, SEM, TEM, XRD, EDAX and particle size analysis techniques revealed the formation of AgNPs with a average particle size of 17.83 nm. The synthesized AgNPs showed good antioxidant activity toward DPPH and also exhibited excellent anti-ageing activity against collagenase enzyme. This investigation provides evidence that AEPR-mediated AgNP synthesis is environmentally benign, moreover, AEPR is anthocyanin rich and contains anti-aging secondary metabolites such as flavonoids and phenolic compounds, making it a potential cosmeceutical ingredient in cosmetic product formulations.

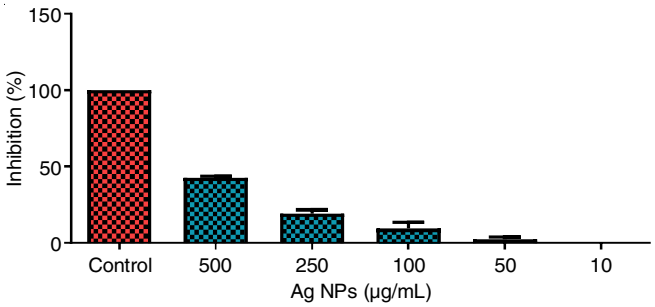


Fig. 11. Percentage of collagenase inhibition by biosynthesized AgNPs

## CONFLICT OF INTEREST

The authors declare that there is no conflict of interests regarding the publication of this article.

## REFERENCES

1. N. Baig, I. Kammakakam and W. Falath, *Mater. Adv.*, **2**, 1821 (2021); https://doi.org/10.1039/D0MA00807A
2. R. Kumar and S. Lal, *J. Nanomater. Mol. Nanotechnol.*, **3**, 11 (2014); https://doi.org/10.4172/2324-8777.1000148
3. S. Mourdikoudis, R.M. Pallares and N.T.K. Thanh, *Nanoscale*, **10**, 12871 (2018); https://doi.org/10.1039/C8NR02278J
4. M.S. Chavali and M.P. Nikolova, *SN Appl. Sci.*, **1**, 607 (2019); https://doi.org/10.1007/s42452-019-0592-3
5. B.H. Alshammari, M.M.A. Lashin, M.A. Mahmood, F.S. Al-Mubaddel, N. Ilyas, N. Rahman, M. Sohail, A. Khan, S.S. Abdullaev and R. Khan, *RSC Adv.*, **13**, 13735 (2023); https://doi.org/10.1039/D3RA01421E
6. G.M. Nair, T. Sajini and B. Mathew, *Talanta Open*, **5**, 100080 (2022); https://doi.org/10.1016/j.talo.2021.100080
7. I. Ijaz, E. Gilani, A. Nazir and A. Bukhari, *Green Chem. Lett. Rev.*, **13**, 223 (2020); https://doi.org/10.1080/17518253.2020.1802517
8. C. Dhand, N. Dwivedi, X.J. Loh, A.N.J. Ying, N.K. Verma, R.W. Beuerman, R. Lakshminarayanan and S. Ramakrishna, *RSC Adv.*, **5**, 105003 (2015); https://doi.org/10.1039/C5RA19388E
9. P. Kuppusamy, M.M. Yusoff, G.P. Maniam and N. Govindan, *Saudi Pharm. J.*, **24**, 473 (2016); https://doi.org/10.1016/j.jsps.2014.11.013
10. N.S.R. Rosman, N.A. Harun, I. Idris and W.I.W. Ismail, *Energy Environ.*, **32**, 1183 (2021); https://doi.org/10.1177/0958305X21989883
11. A. Dhaka, S.C. Mali, S. Sharma and R. Trivedi, *Results Chem.*, **6**, 101108 (2023); https://doi.org/10.1016/j.rechem.2023.101108
12. N.N. Saifuddin, S.N. Matussin, Q. Fariduddin and M.M. Khan, *Bioprocess Biosyst. Eng.*, **47**, 1119 (2024); https://doi.org/10.1007/s00449-024-03044-x

13. F. Arshad, G.A. Naikoo, I.U. Hassan, S.R. Chava, M. El-Tanani, A.A. Aljabali and M.M. Tambuwala, *Appl. Biochem. Biotechnol*., **196**, 3636 (2024); https://doi.org/10.1007/s12010-023-04719-z
14. P.P.N. Vijay Kumar, S.V.N. Pammi, P. Kollu, K.V.V. Satyanarayana and U. Shameem, *Ind. Crops Prod.*, **52**, 562 (2014); https://doi.org/10.1016/j.indcrop.2013.10.050
15. F. Rodríguez-Félix, A.Z. Graciano-Verdugo, M.J. Moreno-Vásquez, I. Lagarda-Díaz, C.G. Barreras-Urbina, L. Armenta-Villegas, A. Olguín-Moreno and J.A. Tapia-Hernández, *J. Nanonater.*, **2022**, 8874003 (2022); https://doi.org/10.1155/2022/8874003
16. D. Tungmunnithum, A. Thongboonyou, A. Pholboon and A. Yangsabai, *Medicines*, **5**, 93 (2018); https://doi.org/10.3390/medicines5030093
17. Y. Zhang, P. Cai, G. Cheng and Y. Zhang, *Nat. Prod. Commun.*, **17**, 1 (2022); https://doi.org/10.1177/1934578X211069721
18. R.G.R. Pinheiro, A.J. Coutinho, M. Pinheiro and A.R. Neves, *Int. J. Mol. Sci*., **22**, 11654 (2021); https://doi.org/10.3390/ijms222111654
19. K.V. Ashwathappa, V. Venkataravanappa, M. Nandan, S. Hiremath, C.N. Lakshminarayana Reddy, K.S. Shankarappa and M.K. Reddy, *Indian Phytopathol.*, **74**, 1065 (2021); https://doi.org/10.1007/s42360-021-00388-2
20. T. Fafal, P. Tastan, B.S. Tüzün, M. Ozyazici and B. Kivcak, *South African J. Botany*, **112**, 346 (2017); https://doi.org/10.1016/j.sajb.2017.06.019
21. S.M. Sheela and J.R. Vimala, *Oriental J. Chem.*, **37**, 984 (2021); https://doi.org/10.13005/ojc/370428
22. N.S. Alharbi, N.S. Alsubhi and A.I. Felimban, *J. Radiat. Res. Appl. Sci*., **15**, 109 (2022); https://doi.org/10.1016/j.jrras.2022.06.012
23. M.I. Skiba, V.I. Vorobyova, A. Pivovarov and N.P. Makarshenko, *J. Nanomater*., **2020**, 3051308 (2020); https://doi.org/10.1155/2020/3051308
24. N.T.K. Thanh, N. Maclean and S. Mahiddine, *Chem. Rev.*, **114**, 7610 (2014); https://doi.org/10.1021/cr400544s
25. R. Veerasamy, T.Z. Xin, S. Gunasagaran, T.F.W. Xiang, E.F.C. Yang, N. Jeyakumar and S.A. Dhanaraj, *J. Saudi Chem. Soc*., **15**, 113 (2011); https://doi.org/10.1016/j.jscs.2010.06.004
26. S.S. Birla, S.C. Gaikwad, A.K. Gade and M.K. Rai, *Scient. World J.*, **2013**, 796018 (2013); https://doi.org/10.1155/2013/796018
27. F.A. Qais, A. Shafiq, H.M. Khan, F.M. Husain, R.A. Khan, B. Alenazi, A. Alsalme and I. Ahmad, *Bioinorg. Chem. Appl.*, **2019**, 4649506 (2019); https://doi.org/10.1155/2019/4649506
28. A. Rahman, G. Rehman, N. Shah, M. Hamayun, S. Ali, A. Ali, S.K. Shah, W. Khan, M.I.A. Shah and A.F. Alrefaei, *Molecules*, **28**, 4203 (2023); https://doi.org/10.3390/molecules28104203
29. V. Ravichandran, S. Vasanthi, S. Shalini, S.A.A. Shah and R. Harish, *Mater. Lett*., **180**, 264 (2016); https://doi.org/10.1016/j.matlet.2016.05.172
30. P. Phanjom, A. Sultana, H. Sarma, J. Ramchiary, K. Goswami and P. Baishya, *Dig. J. Nanomater. Biostruct.*, **7**, 1117 (2012).
31. M. Vanaja and G. Annadurai, *Appl. Nanosci.*, **3**, 217 (2013); https://doi.org/10.1007/s13204-012-0121-9
32. A. Singh, B. Gaud and S. Jaybhaye, *Mater. Sci. Energy Technol.*, **3**, 232 (2020); https://doi.org/10.1016/j.mset.2019.08.004